

# Ultrasensitive and low-cost insole for gait analysis using piezoelectrets

Omar Ben Dali<sup>1</sup>, Youssef Sellami<sup>1</sup>, Sergey Zhukov<sup>2</sup>, Heinz von Seggern<sup>2</sup>,

Niklas Schäfer<sup>1</sup>, Bastian Latsch<sup>1</sup>, Gerhard M. Sessler<sup>1</sup>, Philipp Beckerle<sup>3</sup>, and Mario Kupnik<sup>1</sup>

<sup>1</sup> Measurement and Sensor Technology, Technical University of Darmstadt, Germany.

<sup>2</sup> Electronic Materials, Technical University of Darmstadt, Germany.

<sup>3</sup> Chair of Autonomous Systems and Mechatronics, Friedrich-Alexander-University Erlangen-Nuremberg, Germany.

omar.ben\_dali@tu-darmstadt.de

**Abstract**—The emerging need of wearable healthcare monitoring systems for e.g. predicting cognitive decline, necessitates practical requirements such as high sensor sensitivity and low fabrication costs. In this work, we present an ultrasensitive piezoelectric insole using 3D-printed flexible piezoelectret with a readout circuit that sends measurement data via WiFi. The insole is printed using pure polypropylene filament and consists of eight independent sensors, each with a piezoelectric  $d_{33}$  coefficient of approximately 2000 pC/N. The active part of the insole is protected using a 3D-printed polylactic acid cover that features eight defined embossments on the bottom part, which focus the force on the sensors and act as overload protection against excessive stress. In addition to determining the gait pattern, an accelerometer is implemented to measure kinematic parameters and validate the sensor output signals. The combination of the high sensitivity of the sensors and the kinematic movement of the foot, opens new perspectives regarding diagnosis possibilities through gait analysis.

**Index Terms**—Ferroelectret, piezoelectret, 3D printing, gait analysis.

## I. INTRODUCTION

Healthcare solutions to improve the quality of daily life and to enable early diagnosis of diseases are rapidly gaining in importance. Some neurodegenerative diseases such as Alzheimer's and Huntington's disease have symptoms that involve deficits in gait and balance [1]. Therefore, wearable insoles for gait analysis have become a very active research topic. Various techniques have been proposed including different force measurement principles such as capacitive [2], resistive [3] and piezoelectric insoles [4]. In this context, piezoelectric insoles feature additional advantages compared to the other principles due to their simple structure, high sensitivity and their unique ability to be self-sufficient [5].

Within the category of flexible piezoelectric polymers, piezoelectrets (also known as ferroelectrets) made of cellular polymer foams were first introduced 20 years ago, and feature a large piezoelectric activity of approximately 200 pC N<sup>-1</sup> [6]–[9] outperforming classical PVDF with 25 pC N<sup>-1</sup>.

As a further development step of the cellular polymers, hybrid systems with artificial air-filled voids fabricated through thermoforming, have been intensively studied in recent years

This research received support from the Deutsche Forschungsgemeinschaft (DFG) under grant no. 392020380 and no. 450821862 within the research training group 2761.

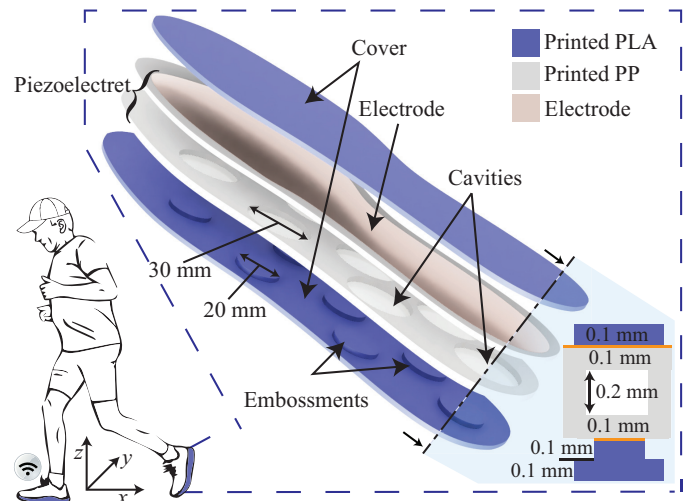


Fig. 1. Schematic representation of the smart insole embedded in a person shoes. The exploded-view of the insole displays two grey layers consisting of printed PP, that form together the piezoelectret. The two outer blue layers consist of PLA and present the cover of the piezoelectret.

[10]–[14]. These artificial piezoelectrets feature a piezoelectric activity that depends on the voids geometry. Thereby, very large longitudinal piezoelectric  $d_{33}$  coefficients up to 23 000 pC N<sup>-1</sup> were achieved [15].

Due to the large piezoelectric coefficients and mechanical flexibility of such materials, they were used in several energy harvesting devices [16]–[21] and even reached a normalized output power up to 1 mW [22].

Recently, 3D-printing of piezoelectrets as a new manufacturing route has been investigated using known electret materials such as polypropylene (PP) [23], acrylonitrile butadiene styrene (ABS) [24] and polylactic acid (PLA) [25], [26]. It has been shown that through a proper void geometry, large piezoelectric  $d_{33}$  coefficient up to 600 pC N<sup>-1</sup> can be achieved [26].

In this work, we present a flexible 3D printed insole consisting of an active layer sandwiched between two cover-layers. The active layer is printed using PP and exhibits eight cavities that can be treated to act as independent piezoelectric sensors.

The insole is tested regarding the piezoelectric response of each sensor and its applicability in gait analysis. The main focus hereby is providing a very sensitive, low-cost and self-sufficient insole for gait analysis, and, thus, also health monitoring.

## II. PREPARATION OF THE INSOLE

The piezoelectret, which is the active part of the insole, is printed using polypropylene (PP) and exhibits eight well defined circular cavities, each with 30 mm diameter. Due to the large diameter of the cavities, bridging them results in undefined sagging of the printed lines, thus hindering the charging process. Therefore, the piezoelectret is assembled from two independently printed parts. The first part is 0.3 mm thick, with cavities of 0.2 mm and the second part is an unstructured plane-parallel film (Fig. 1). The two parts are subsequently thermal-bonded and together form the piezoelectret structure. The insole geometry is designed in Autodesk Fusion 360 (Autodesk, Inc) and prepared for 3D printing using an open source software (Slic3r). The latter divides the 3D model into layers defined as movements of the three axis of the 3D printer (Prusa Mk3s, Prusa3d DE). Each printed layer is 0.1 mm thick, using a printing speed of  $5 \text{ mm s}^{-1}$ . The nozzle diameter is 0.4 mm that extrudes fused PP-filament (Formfutura BV) on a spring steel sheet with smooth double-sided Polyetherimide (PEI) as the printing bed.

The assembled insole is then provided with a large-area electrode on the outer side of the flat PP film and eight electrodes on the outer side of the structured PP film (Fig. 1). The eight electrodes feature a diameter of 20 mm and are placed on top of the eight cavities.

The polarization of the structure is carried out under ambient conditions by applying a DC voltage of  $-7 \text{ kV}$  (power supply HCN 350-20000, fug Elektronik GmbH) on each sensor, resulting in large electric fields in the air-filled cavities. When these electric fields exceed the breakdown electric field strength  $E_B$  in air, a Paschen breakdown [27] is initialized generating micro-dipoles between the two polymer walls. The positive and negative charges remain quasi-permanently trapped and form the piezoelectret [Fig. 2(a)]. The charged insole is then placed between two 3D-printed PLA layers as a cover. The printing parameters of PLA filament have been reported in previous publications [25], [26].

The bottom layer of the cover features eight embossments in order to maximize the force on the active area while walking. Each embossment features a diameter of 20 mm, which corresponds to the electrodes diameter (Fig. 1) and a thickness of 0.1 mm. The thickness of the embossments limits the maximum possible deformation under an external load. This also serves as a safeguard as well since the weight of individual persons can vary significantly. The top layer of the cover, on the other hand, is flat to ensure the comfort of the person walking.

## III. CHARACTERIZATION OF THE INSOLE AND MEASUREMENT CIRCUIT

The piezoelectric response is characterized by measuring the  $d_{33}$  coefficient of each sensor using the quasi-static method. First a mass of 200 g and 20 mm diameter is applied to the sensor for an extended period of time (3 min). After removing the mass, the previously induced charge is measured by means of an electrometer (6517A, Keithley Instruments) and integrated over 10 s. The measured piezoelectric  $d_{33}$  coefficient of all sensors is approximately  $2000 \text{ pC N}^{-1}$ . This value, however is only valid for small loads up to approximately 10 N. A larger deformation than 0.1 mm is restrained by the contact of the large surface of the cover with the rigid surface of the piezoelectret [Fig. 2(a)]. Note that a discharge of the films has not been observed in the case of contact. An increase of the load still deforms the entire structure since the polymers compress, although with a much smaller amplitude compared to the initial deformation of the air cavities.

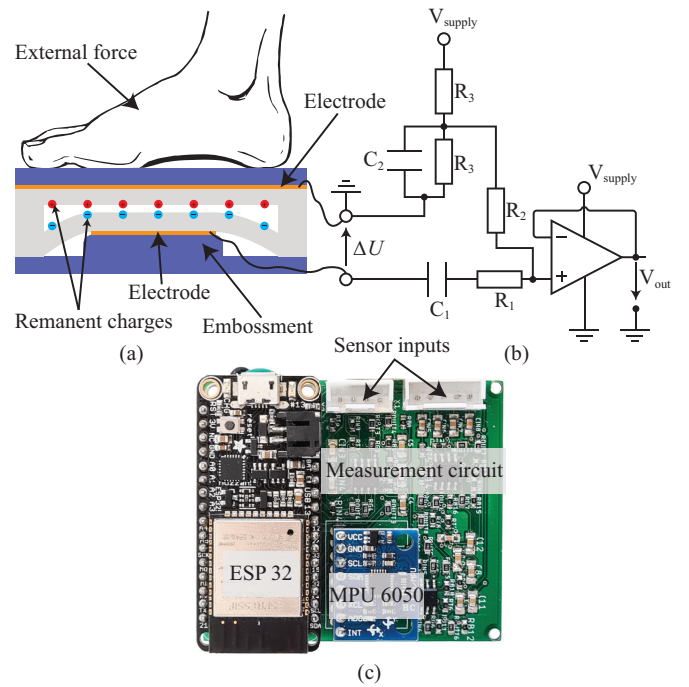


Fig. 2. Scheme of the gait analysis: (a) Illustration of a deformed cavity when an external force is applied to the insole, (b) measurement circuit of one sensor using single supply operational amplifier design and (c) the used hardware consisting of the measurement circuit of all eight sensors, an accelerometer (MPU 6050) and a microcontroller (ESP32 Feather Board).

In view of its practical interest as sensor for gait analysis, a measurement circuit is designed, that measures the individual voltages of the sensors when a force is applied (Fig. 2). The output voltage of each sensor is measured through the voltage divider  $R_1$  and  $R_2$  [Fig. 2(b)]. The capacitor  $C_1$  is a coupling capacitor that acts as DC blocking component and  $C_2$  is used to bypass the ac signals appearing on the supply line. For the single supply configuration an artificial zero-signal reference voltage is fixed between the supply rails using the voltage divider consisting of two resistors  $R_3$ . The same

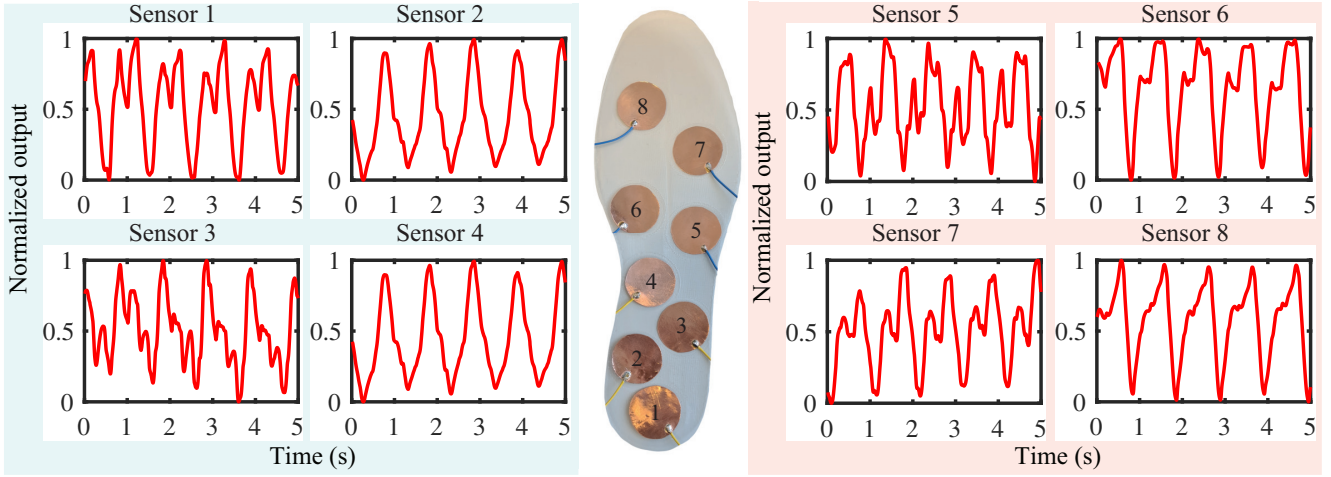


Fig. 3. Normalized output voltages of the eight sensors of the insole corresponding to the signal generated by a walking 60 kg male of foot size 40. The heel part includes the sensors from one to four and their signals are shown on a blue background. The forefoot area include the sensors from five to eight and their signals are shown on a red background.

resistor  $R_3$  is used to establish the bias at the midpoint of the supply voltage. The output voltages of all eight operational amplifiers are converted to digital signals through an analog-digital-converter (MCP3008), which transmits the sensors data to the microcontroller ESP32 through the Serial Peripheral Interface (SPI). The ESP32 in turn sends the measured data to a computer as a data receiver using the communication protocol User Datagram Protocol (UDP). The MPU6050 is an accelerometer and gyroscope which is used to track and validate the walking steps. Further signal processing of the data is beyond the scope of this paper and will be published separately.

#### IV. EXPERIMENTAL RESULTS OF THE GAIT ANALYSIS

The measurement results correspond to a walking 60 kg male of foot size EU 40 (Fig. 3). An enumeration of the sensor locations is given to compare the sensors of the insole, which helps allocating the measurement results to their corresponding measured sensor. The sensors placed on the heel part of the foot are enumerated from 1 to 4 and the ones placed on the forefoot from 5 to 8.

One stride can be divided into two major phases, i.e. stance phase and swing phase [28]. The transition from swing phase to stance phase (heel-strike) corresponds to stressing the sensors whereas the opposite transition (toe-off) marks the release. The stressing results in negative voltage output of all sensors whereas the release results in a positive output voltage. The polarity of the output voltage depends on the utilized charging polarity of the sensors. The maximum strike of one sensor corresponds to approximately 150 V which is converted to 3.3 V on the measurement board. However, since the focus of this work lies solely on detecting the movement, only the normalized output signals are considered.

The shapes of the sensor signals differ from each other due to the different load types while walking (Fig. 3). In

the present case, Sensor 1 shows first an increasing voltage followed by the main strike. The increasing voltage matches the contact of the edge of the heel with the ground resulting in a small inclination of the insole. The inclination acts as stressing the sensor in the positive  $z$ -direction leading to a positive output voltage. Afterwards, the heel stresses the sensor in the negative  $z$ -direction and causes the main strike presented by the negative voltage peak. Further movement forward first releases sensor 1 and then inclines the insole one more time. This results in an overlap of the two deformation stages which can be seen at the signal shape.

Sensor 4 is placed under the arch of the foot resulting in smaller deflections and larger release signals. The amplitude of the strikes of this sensor depends on the arch of foot. A flatfoot would result in larger strikes.

The last sensor to be stressed when moving forward is Sensor 8. The effect of first releasing the sensor followed by the strike can be seen with a time delay. If only the time delay between strikes is considered, moving forward and backwards can be detected. If the magnitude of the strikes is as well considered, walking and running can be distinguished from each other.

#### V. CONCLUSION AND OUTLOOK

In this work, we designed an ultrasensitive insole using ferroelectret based mechanical sensor. 3D-printing the insole with well-defined artificial cavities broadens the possibilities of piezoelectric insole design. Designing more complex structures using 3D printing techniques is a field with great potential. In this context, different application fields can be incorporated by designing custom insole with adjustable local sensitivities. The readout circuit suggested is simple and consists of low-cost discrete components, which is an additional advantage of using piezoelectric sensors.

## REFERENCES

- [1] G. Ciciirelli, D. Impedovo, V. Dentamaro, R. Marani, G. Pirlo, and T. D’Orazio, “Human gait analysis in neurodegenerative diseases: A review,” *IEEE Journal of Biomedical and Health Informatics*, 2021.
- [2] M. Ntagios and R. Dahiya, “3d printed soft and flexible insole with intrinsic pressure sensing capability,” *IEEE Sensors Journal*, 2022.
- [3] J. S. Park, C. M. Lee, S.-M. Koo, and C. H. Kim, “Gait phase detection using force sensing resistors,” *IEEE Sensors Journal*, vol. 20, no. 12, pp. 6516–6523, 2020.
- [4] J. Chen, Y. Dai, S. Kang, L. Xu, and S. Gao, “A concurrent plantar stress sensing and energy harvesting technique by piezoelectric insole device and rectifying circuitry,” *IEEE Sensors Journal*, vol. 21, no. 23, pp. 26 364–26 372, 2021.
- [5] Y. Xin, X. Li, H. Tian, *et al.*, “Shoes-equipped piezoelectric transducer for energy harvesting: A brief review,” *Ferroelectrics*, vol. 493, no. 1, pp. 12–24, 2016.
- [6] S. Bauer, R. Gerhard, and G. M. Sessler, “Ferroelectrets : Soft electroactive foams for transducers,” 2004.
- [7] M. Wegener and S. Bauer, “Microstorms in cellular polymers: A route to soft piezoelectric transducer materials with engineered macroscopic dipoles,” *Chemphyschem : a European journal of chemical physics and physical chemistry*, vol. 6, no. 6, pp. 1014–1025, 2005.
- [8] M. Paajanen, J. Lekkala, and K. Kirjavainen, “Electromechanical film (emfi) — a new multipurpose electret material,” *Sensors and Actuators A: Physical*, vol. 84, no. 1-2, pp. 95–102, 2000.
- [9] G. S. Neugschwandtner, R. Schwödiauer, M. Vieytes, *et al.*, “Large and broadband piezoelectricity in smart polymer-foam space-charge electrets,” *Applied Physics Letters*, vol. 77, no. 23, pp. 3827–3829, 2000.
- [10] R. Altafim, H. Basso, R. Altafim, *et al.*, “Piezoelectrets from thermo-formed bubble structures of fluoropolymer-electret films,” *IEEE Transactions on Dielectrics and Electrical Insulation*, vol. 13, no. 5, pp. 979–985, 2006.
- [11] R. A. P. Altafim, X. Qiu, W. Wirges, *et al.*, “Template-based fluoroethylenepropylene piezoelectrets with tubular channels for transducer applications,” *Journal of Applied Physics*, vol. 106, no. 1, p. 014 106, 2009.
- [12] Z. Sun, X. Zhang, Z. Xia, *et al.*, “Polarization and piezoelectricity in polymer films with artificial void structure,” *Applied Physics A*, vol. 105, no. 1, pp. 197–205, 2011.
- [13] S. Zhukov, D. Eder-Goy, C. Biethan, S. Fedosov, B.-X. Xu, and H. von Seggern, “Tubular fluoropolymer arrays with high piezoelectric response,” *Smart Materials and Structures*, vol. 27, no. 1, p. 015 010, 2017.
- [14] X. Ma, H. von Seggern, G. M. Sessler, *et al.*, “High performance fluorinated polyethylene propylene ferroelectrets with an air-filled parallel-tunnel structure,” *Smart Materials and Structures*, vol. 30, no. 1, p. 015 002, 2020.
- [15] H. von Seggern, S. Zhukov, O. Ben Dali, C. Hartmann, G. M. Sessler, and M. Kupnik, “Highly efficient piezoelectrets through ultra-soft elastomeric spacers,” *Polymers*, vol. 13, no. 21, p. 3751, 2021.
- [16] J. Shi, S. Yong, and S. Beeby, “An easy to assemble ferroelectret for human body energy harvesting,” *Smart Materials and Structures*, vol. 27, no. 8, p. 084 005, 2018.
- [17] Y. Wang, L. Wu, and X. Zhang, “Energy harvesting from vibration using flexible fluoroethylenepropylene piezoelectret films with cross-tunnel structure,” *IEEE Transactions on Dielectrics and Electrical Insulation*, vol. 22, no. 3, pp. 1349–1354, 2015.
- [18] Y. Zhang, C. R. Bowen, S. K. Ghosh, *et al.*, “Ferroelectret materials and devices for energy harvesting applications,” *Nano Energy*, vol. 57, pp. 118–140, 2019.
- [19] O. Ben Dali, S. Zhukov, R. Chadda, *et al.*, “Modeling of piezoelectric coupling coefficients of soft ferroelectrets for energy harvesting,” in *2019 IEEE International Ultrasonics Symposium (IUS)*, IEEE, 6.10.2019 - 09.10.2019, pp. 2454–2457.
- [20] S. Zhukov, H. von Seggern, X. Zhang, *et al.*, “Microenergy harvesters based on fluorinated ethylene propylene piezotubes,” *Advanced Engineering Materials*, vol. 22, no. 5, p. 1901 399, 2020.
- [21] O. Ben Dali, P. Pondrom, G. M. Sessler, *et al.*, “Cantilever-based ferroelectret energy harvesting,” *Applied Physics Letters*, vol. 116, no. 24, p. 243 901, 2020.
- [22] O. Ben Dali, H. von Seggern, G. M. Sessler, *et al.*, “Ferroelectret energy harvesting with 3d-printed air-spaced cantilever design,” *Nano Select*, vol. 3, no. 3, pp. 713–722, 2022.
- [23] N. Wang, K. Davis, M. Sotzing, *et al.*, “Flexible nanogenerator with 3d-printed ferroelectrets,” in *2021 IEEE Conference on Electrical Insulation and Dielectric Phenomena (CEIDP)*, IEEE, 2021, pp. 375–378.
- [24] I. Kierzewski, S. S. Bedair, B. Hanrahan, H. Tsang, L. Hu, and N. Lazarus, “Adding an electroactive response to 3d printed materials: Printing a piezoelectret,” *Additive Manufacturing*, vol. 31, p. 100 963, 2020.
- [25] O. Ben Dali, S. Zhukov, M. Rutsch, *et al.*, “Biodegradable 3d-printed ferroelectret ultrasonic transducer with large output pressure,” in *2021 IEEE International Ultrasonics Symposium (IUS)*, IEEE, 2021, pp. 1–4.
- [26] O. Ben Dali, S. Zhukov, C. Hartman, H. von Seggern, G. M. Sessler, and M. Kupnik, “Biodegradable additive manufactured ferroelectret as mechanical sensor,” in *2021 IEEE Sensors*, IEEE, pp. 1–4.
- [27] B. H. Crichton, “Gas discharge physics,” in *Gas discharge physics*, IET, 4 Oct. 1996, p. 3.
- [28] M. W. Whittle, “Gait analysis,” in *The soft tissues*, Elsevier, 1993, pp. 187–199.